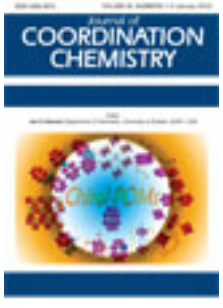

Journal of Coordination Chemistry
Publication details, including instructions for authors and subscription information:
http://www.tandfonline.com/loi/gcoo20

Synthesis, DNA-binding, cytotoxicity, and cleavage studies of unsymmetrical oxovanadium complexes

Haiwei Guo [a], Jiazheng Lu [a], Zhigang Ruan [b], Yongli Zhang [b], Yunjin Liu [a], Linquan Zang [a], Jing Jiang [a c] & Jinwang Huang [c]

[a] School of Pharmacy, Guangdong Pharmaceutical University, Guangzhou 510006, People's Republic of China

[b] School of Basic Courses, Guangdong Pharmaceutical University, Guangzhou 510006, People's Republic of China

[c] State Key Laboratory of Optoelectronic Material and Technologies & School of Chemistry and Chemical Engineering, Sun Yat-Sen University, Guangzhou 510275, People's Republic of China

Published online: 21 Dec 2011.

To cite this article: Haiwei Guo, Jiazheng Lu, Zhigang Ruan, Yongli Zhang, Yunjin Liu, Linquan Zang, Jing Jiang & Jinwang Huang (2012) Synthesis, DNA-binding, cytotoxicity, and cleavage studies of unsymmetrical oxovanadium complexes, Journal of Coordination Chemistry, 65:2, 191-204, DOI: 10.1080/00958972.2011.645204

To link to this article: http://dx.doi.org/10.1080/00958972.2011.645204

Journal of Coordination Chemistry
Vol. 65, No. 2, 20 January 2012, 191–204

Synthesis, DNA-binding, cytotoxicity, and cleavage studies of unsymmetrical oxovanadium complexes

HAIWEI GUO†, JIAZHENG LU*†, ZHIGANG RUAN‡, YONGLI ZHANG‡, YUNJIN LIU†, LINQUAN ZANG†, JING JIANG†§ and JINWANG HUANG§

†School of Pharmacy, Guangdong Pharmaceutical University, Guangzhou 510006, People's Republic of China
‡School of Basic Courses, Guangdong Pharmaceutical University, Guangzhou 510006, People's Republic of China
§State Key Laboratory of Optoelectronic Material and Technologies & School of Chemistry and Chemical Engineering, Sun Yat-Sen University, Guangzhou 510275, People's Republic of China

(*Received 5 September 2011; in final form 11 November 2011*)

An unsymmetrical oxovanadium complex [VO(SAA)(phen)] (**1**) (SAA = salicylidene anthranilic acid, phen = phenanthroline) and its derivative [VO(MOSAA)(phen)] (**2**) (MOSAA = 2-hydroxy-4-methoxysalicylidene anthranilic) have been synthesized and characterized by elemental analysis, UV-Vis, ES-MS, IR, and ^{1}H NMR. The interaction of these two complexes with calf thymus DNA (CT-DNA) was investigated by absorption titration, fluorescence spectra, viscosity measurements, and thermal denaturation. Their photocleavage reactions with pBR322 supercoiled plasmid DNA were investigated by gel electrophoresis. The cytotoxicity of these two complexes against myeloma cell (Ag8.653) and gliomas cell (U251) have been assessed by MTT assay. The results show that both **1** and **2** bind to CT-DNA in classical intercalation, and the DNA-binding affinity of **1** is larger than that of **2**. These complexes enhance the oxidative cleavage of supercoiled pBR322 DNA and both complexes have cytotoxic activities against Ag8.653 and U251 cell lines. Complex **1** has more potent inhibitory effect against the two cell lines than **2**.

Keywords: Oxovanadium complexes; DNA-binding; Cytotoxicity; Cleavage

1. Introduction

Transition metal complexes have been exploited for design of new drugs due to their diverse biological activities. Most of these properties have been found to arise from complexes binding DNA and cleaving DNA [1–3]. DNA-binding metal complexes, especially those with small molecular weight, have been extensively studied as DNA structural and conformational probes, DNA-dependent electron transfer and sequence-specific cleaving agents, and potential anti-cancer drugs [4–6].

*Corresponding author. Email: lujia6812@163.com

ISSN 0095-8972 print/ISSN 1029-0389 online
http://dx.doi.org/10.1080/00958972.2011.645204

Vanadium complexes have antibacterial, antitumor, insulin-enhancing, and antiparasitic effects [7–10]. Vanadium takes part in various DNA maintenance reactions and thereby prevents genomicin stability which otherwise leads to cancer [11–15]. Vanadium complexes also suppress the growth and spread of existing tumors by inhibiting tumor cell proliferation, inducing apoptosis, and limiting the invasion and metastatic potential of neoplastic cells. Thus, DNA-binding and antitumor activities of oxovanadium complexes and multifunctional bridging ligands have been investigated [8, 9]. Schiff bases have been extensively studied because of their potential antibacterial, antifungal, anti-malarial, and anticancer activities [10, 13, 16]. In this context, salicylidene anthranilic acid (SAA) and its derivative are chosen as ligands for oxovanadium complexes. The presence of a rigid aromatic system in the Schiff base structure gives particular spectroscopic properties, which make it a potential probe for nucleic acids. Electronic effects of Schiff-base complexes are important in this field in order to design complexes with better DNA-binding characteristics [11, 17]. Increasing interest in chemistry of Schiff base derivatives has prompted development of efficient synthetic procedures for functionalization at the various ring positions of Schiff bases which involves phen. Relatively simple Schiff-base ligands are building blocks for various purposes, as well as new intercalating agents for polynucleotides [16–19].

Previously, we studied the interactions of some oxovanadium complexes, [VO(satsc)(bipy)] (satsc = salicylaldehyde thiosemicarbazone; bipy = 2,2′-bipyridine) and its derivative [VO(3,5-dibrsatsc)(bipy)] (3,5-dibrsatsc = 3,5-dibromosalicylaldehyde thiosemicarbazone) with calf thymus DNA (CT-DNA), and found that these oxovanadium complexes interact with CT-DNA through intercalation [18, 19]. In continuation of our investigations of biological activities of oxovanadium complexes, we synthesized and characterized two other oxovanadium complexes, [VO(SAA)(phen)] (**1**) (phen = 1,10-phenanthroline) and [VO(MOSAA)(phen)] (**2**) (MOSAA = 2-hydroxy-4-methoxysalicylidene anthranilic; phen = 1,10-phenanthroline), scheme 1. The DNA-binding behaviors of the two complexes were explored by absorption titration, fluorescence spectra, viscosity measurements, and thermal denaturation. Their photocleavage reactions with pBR322 supercoiled plasmid DNA were investigated by gel electrophoresis. The cytotoxicity of these two complexes against the myeloma cell (Ag8.653) and gliomas cell (U251) were assessed by MTT assay.

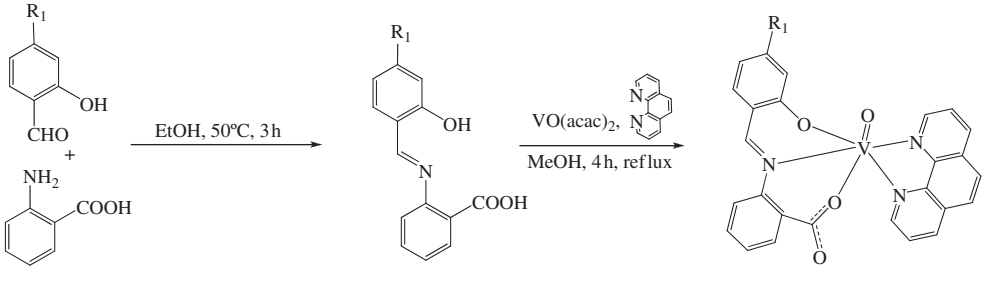

(**1**): $R_1 = H$
(**2**): $R_1 = CH_3O$

Scheme 1. The synthetic routes for ligands and complexes.

2. Experimental

2.1. *Materials*

$VO(acac)_2$ (acac = acetylacetonate) and 1,10-phenanthroline were purchased from Shanghai Jingchun company. CT-DNA and pBR 322 DNA were obtained from Sigma. Other materials were obtained from commercial sources and used as received (analytical reagents). Tris-HCl buffer A (5 mmol L^{-1} Tris (hydroxymethylaminomethane)-HCl, 50 mmol L^{-1} NaCl, pH = 7.2) was used for absorption titration, luminescence titration, and viscosity experiments. Tris-HCl buffer B (50 mmol L^{-1} Tris-HCl and 18 mmol L^{-1} NaCl, pH = 7.2) was used for DNA-cleavage experiments. Buffer C (1.5 mmol L^{-1} $NaHPO_4$, 0.5 mmol L^{-1} NaH_2PO_4, and 0.25 mmol L^{-1} Na_2H_2EDTA = (H_4EDTA = *N*,*N*′-ethane-1,2-diylbis[*N*-(carboxymethyl)glycine]) (pH = 7.0) was used for thermal denaturation. All buffers were prepared using doubly distilled water. A solution of CT-DNA in the buffer gave a ratio of UV absorbance at 260 and 280 nm of *ca* 1.8–1.9, indicating that the DNA was sufficiently free of protein [18–20]. The DNA concentration per nucleotide was determined by absorption spectroscopy using the molar absorption coefficient (6600 $(mol\,L^{-1})^{-1}\,cm^{-1}$) at 260 nm [19, 21].

2.1.1. Synthesis of SAA. SAA was synthesized through modification of a previously reported procedure [18, 19]. A stirring solution of salicylaldehyde (521 μL, 5 mmol) in 10 cm^3 of absolute alcohol was added dropwise to anthranilic acid (0.686 g, 5 mmol) which was dissolved in 10 cm^3 of absolute alcohol; the mixture was continuously stirred at 50°C for 3 h giving a pink precipitate. Yield: 57%. Anal. Calcd for $C_{14}H_{11}NO_3$ (%): C, 69.70; H, 4.60; N, 5.81; Found (%): C, 69.61; H, 4.79; N, 5.74. ES-MS (CH_3OH, *m*/*z*): 242.0 ($[M+1]^+$). UV, λ_{max}, nm (ε, $(mol\,L^{-1})^{-1}\,cm^{-1}$) in DMSO: 258 (34,300), 338 (30,150). IR (KBr)(ν_{max}/cm^{-1}): 3500 (br) (OH), 3069, 3039 (m, ArH), 1682 (s) (COOH), 1618 (vs) (C=N + C=C), 1570 (s) (C=C), 1457 (m) (C=C), 1389 (m), 1363 (s), 1242 (vs) (C–O), 811 (s), 756 (vs), 678 (s), 576 (m), 486 (s). ^1H NMR (500 MHz, DMSO-d_6): 13.05 (br s, 1H, COOH), 10.27 (s, 1H, OH), 8.87 (s, 1H, –CH=N–), 7.87 (s, 1H, ArH), 7.65 (d, 1H, ArH, *J* = 8.2 Hz), 7.52 (t, 1H, ArH, *J* = 8.7 Hz), 7.46 (s, 1H, ArH), 7.22 (t, 1H, ArH), 6.97 (t, 1H, ArH, *J* = 8.0 Hz), 6.74 (d, 1H, ArH, *J* = 8.4 Hz), 6.50 (t, 1H, ArH, *J* = 7.8 Hz).

2.1.2. Synthesis of MOSAA. This ligand was prepared using a similar procedure described for SAA, but from 4-methoxysalicylaldehyde (0.761 g, 5 mmol). Yield: 65%. Anal. Calcd for $C_{15}H_{13}NO_4$ (%): C, 66.41; H, 4.83; N, 5.16; Found (%): C, 66.33; H, 4.97; N, 5.10. ES-MS (CH_3OH, *m*/*z*): 272.0 ($[M+1]^+$). UV, λ_{max}, nm (ε, $(mol\,L^{-1})^{-1}\,cm^{-1}$) in DMSO: 257 (13,350), 340 (29,250). IR (KBr)(ν_{max}/cm^{-1}): 3470 (br) (OH), 3055 (m) (ArH), 2951 (m), 2847 (w) (CH_3O–), 1697 (s) (COOH), 1615 (br, vs) (C=N + C=C), 1564 (s) (C=C), 1514 (C=C), 1457 (m) (C=C), 1392 (m) (–CH_3), 1359 (s), 1267 (vs) (COOH), 1240 (s) (C–O), 1022 (s), 841 (s), 784 (m), 762 (s), 732 (m), 671 (s), 601 (m), 483 (s). ^1H NMR (500 MHz, DMSO-d_6): 13.31 (br s, 1H, COOH), 10.02 (s, 1H, OH), 8.76 (s, 1H, –CH=N–), 7.88 (d, 1H, ArH, *J* = 8.2 Hz), 7.63 (t, 1H, ArH, *J* = 8.0 Hz), 7.54 (d, 1H, ArH, *J* = 7.9 Hz), 7.46 (d, 1H, ArH, *J* = 8.4 Hz),

7.34 (t, 1H, ArH, $J = 8.2$ Hz), 6.55 (d, 1H, ArH, $J = 7.8$ Hz), 6.48 (d, 1H, ArH, $J = 8.0$ Hz), 3.82 (s, 3H, CH_3O–).

2.1.3. Synthesis of [VO(SAA)(phen)] (1). A mixture of SAA (0.121 g, 0.5 mmol) and 1,10-phenanthroline (0.090 g, 0.5 mmol) in absolute methanol (15 cm^3) was heated at 80°C under argon for 2 h. After dissolution, a 10 cm^3 methanolic solution of $VO(acac)_2$ (0.1325 g, 0.5 mmol) was added dropwise to this mixture. The mixture was refluxed for another 4 h to give a reddish-brown precipitate. Then the solid powder was filtered from the hot solution, washed with absolute methanol and diethyl ether, respectively, and dried in vacuum. Yield: 80.4%. Anal. Calcd for $C_{26}H_{17}N_3O_4V$ (%): C, 64.19; H, 3.52; N, 8.64; Found (%): C, 62.24; H, 3.77; N, 8.36. Ω_M ($\Omega^{-1}\,cm^2\,mol^{-1}$, in DMF): 19.9. ES-MS ($CH_3OH$, m/z): 487.0 ($[M+1]^+$). UV, λ_{max}, nm (ε, $(mol\,L^{-1})^{-1}\,cm^{-1}$) in DMSO: 264.5 (34,150), 404 (5200). IR (KBr)(ν_{max}/cm^{-1}): 3062 (w) (ArH), 3014 (w) (ArH), 1601 (vs) (C=N + C=C), 1531 (s) (C=C), 1433 (s) (C=C), 1383 (m), 1349 (m), 1217 (w) (C–O), 1180 (w), 1146 (m), 964 (s) (VO), 873 (m), 846 (m), 771 (m), 721 (m), 611 (w), 559 (w), 538 (w), 465 (w). ^1H NMR (500 MHz, DMSO-d_6): 9.08 (s, 1H, –CH=N–), 8.13–8.49 (m, 7H, ArH), 8.00 (s, 2H, ArH), 7.77 (s, 1H, ArH), 6.50–7.32 (br m, 6H, ArH). Magnetic moment: μ_{eff}: 1.69 BM.

2.1.4. Synthesis of [VO(MOSAA)(phen)] (2). This complex was prepared using a similar procedure described for **1**. Yield: 84.7%. Anal. Calcd for $C_{27}H_{19}N_3O_5V$ (%): C, 62.80; H, 3.71; N, 8.14; Found (%): C, 62.51; H, 3.92; N, 8.09. Ω_M ($\Omega^{-1}\,cm^2\,mol^{-1}$): 21.0. ES-MS ($CH_3OH$, m/z): 517.0 ($[M+1]^+$). UV, λ_{max}, nm (ε, $(mol\,L^{-1})^{-1}\,cm^{-1}$) in DMSO: 264 (36,400), 370 (4950). IR (KBr)(ν_{max}/cm^{-1}): 3063 (w) (ArH), 1597 (vs) (C=N + C=C), 1512 (s) (C=C), 1421 (w) (C=C), 1375 (m), 1326 (s), 1225 (s) (C–O), 1180 (s), 1114 (s), 1024 (w), 970 (s) (VO), 852 (m), 766 (m), 721 (m), 553 (w), 539 (w), 420 (w). ^1H NMR (500 MHz, DMSO-d_6): 9.11 (s, 1H, –CH=N–), 8.36–8.49 (m, 8H, ArH), 7.99 (s, 2H, ArH), 7.79 (s, 2H, ArH), 6.48–6.96 (br m, 3H, ArH), 3.71 (s, 3H, CH_3O). Magnetic moment: μ_{eff}: 1.73 BM.

2.2. *Physical measurements*

Microanalyses (C, H, and N) were carried out with a Perkin-Elmer 240Q elemental analyzer. Electrospray mass spectra (ES-MS) were recorded on a LCQ system (Finnigan MAT, USA) using methanol as mobile phase. ^1H NMR spectra were recorded on a Varian-500 spectrometer with chemical shifts given relative to tetramethylsilane (TMS). Infrared (IR) spectra were recorded on a Perkin-Elmer Lambda 35 instrument using KBr pellets. UV-Vis spectra were recorded on a Shimadzu UV-3101 PC spectrophotometer at room temperature. Emission spectra were recorded on a Perkin-Elmer Lambda 55 spectrofluorophotometer. Molar conductivities were measured using a DDS-307 digital direct reading conductivity meter in DMF solution (1 mmol L^{-1}) at room temperature. Magnetic susceptibility measurements were recorded on an MPMSXL-7 (Quantum Design, USA) at room temperature.

2.3. *DNA-binding and cleavage experiments*

Absorption titration experiments were performed with fixed concentration of the complexes (20 μmol L^{-1}) while gradually increasing the concentration of CT-DNA. V-DNA solutions were allowed to incubate for 5 min before the absorption spectra were recorded. In order to compare the binding strength of the complexes, their intrinsic binding constants (K_b) were determined by monitoring changes of absorbance in the ligand transfer band with increasing concentrations of CT-DNA. K_b was then calculated using the following equation [18, 22, 23]:

$$\frac{[DNA]}{\varepsilon_a - \varepsilon_f} = \frac{[DNA]}{\varepsilon_b - \varepsilon_f} + \frac{1}{K_b(\varepsilon_b - \varepsilon_f)}, \quad (1)$$

where [DNA] is the concentration of DNA in the base pairs, ε_a is the extinction coefficient observed for $A_{obsd}/[V]$, ε_b is the extinction coefficient of the complex when fully bound to DNA, ε_f is the extinction coefficient of the complex free in solution. The non-linear least-squares analysis was done using Origin Lab, version 7.5.

Viscosity measurements were carried out with an Ubbelohde viscometer maintained at a constant temperature (28 ± 0.1)°C in a thermostatic bath. A digital stopwatch was used for flow time and each sample was measured five times to obtain the average flow time. Data are presented as $(\eta/\eta_0)^{1/3}$ *versus* binding ratio, where η is the viscosity of DNA in the presence of complexes while η_0 is the viscosity of DNA alone [18, 24].

Thermal denaturation studies were carried out with a Shimadzu UV-3101 PC spectrophotometer equipped with a Peltier temperature-controlling programmer (±0.1°C). The melting curves were obtained by measuring the absorbance at 260 nm for solutions of CT-DNA (80 μmol L^{-1}) in the absence and presence of oxovanadium complex (20 μmol L^{-1}) as a function of temperature. The temperature was scanned from 50°C to 90°C at a speed of 5°C min^{-1}.

The cleavage of supercoiled pBR322 DNA by the complexes was studied by gel electrophoresis; pBR322 DNA (0.1 μg) was treated with the oxovanadium complexes in buffer B, and the solution was incubated at 37°C in the incubator. The samples were analyzed by electrophoresis for 1.5 h at 85 V on a 0.8% agarose gel in TBE (89 mmol L^{-1} Tris-borate acid, 2 mmol L^{-1} EDTA, pH = 8.3). The gel was stained with 1 μg mL^{-1} ethidium bromide and photographed on an Alpha Innotech IS-5500 fluorescence chemiluminescence and visible imaging system [2, 18, 19, 25].

2.4. *Cell viability assay*

The capacities of compounds to interfere with the growth of myeloma cells (Ag8.653) and gliomas cells (U251) were determined with the aid of MTT dye assay. Compounds were dissolved in DMSO and diluted with RPMI 1640 to the required concentrations prior to use. The control was prepared by addition of culture medium (100 μL). Wells containing culture medium without cells were used as blanks. Myeloma cells (Ag8.653) and gliomas cells (U251) with a density 2×10^4 cells per well were seeded in 96-well microtiter plates and then treated with varying doses of the vanadium complex and the reference drug cisplatin in a highly humidified atmosphere of 95% air with 5% CO_2 at 37°C for 48 h. For each of the variants tested, four wells were used. Upon completion of the incubation, stock MTT dye solution was added to each well. After 4 h incubation,

a solution containing DMF (50%) sodium dodecyl sulfate (20%) was added to solubilize the MTT formazan. The cell viability was determined by measuring the absorbance of each well at 490 nm using a Multiskan SSCENT microplate reader. IC_{50} values were determined by plotting the percentage viability *versus* concentration on a logarithmic graph and reading off the concentration at which 50% of cells remain viable relative to the control [17, 26, 27].

3. Results and discussion

3.1. *Synthesis and characterization*

The ligands SAA and 4-CH_3O-SAA were prepared by the reaction of anthranilic acid with salicylaldehyde and 4-methoxysalicyladehyde, respectively, in the appropriate mole ratios using absolute ethanol as solvent [19, 27]. The complexes [VO(SAA)(phen)] (**1**) and [VO(MOSAA)(phen)] (**2**) were prepared by refluxing of corresponding ligand, $VO(acac)_2$ and 1,10-phenanthroline in absolute methanol. The desired complexes were purified by recrystallization. The structures of ligand and its corresponding complexes were confirmed by elemental analysis, ES-MS, IR, and ^1H NMR spectroscopies. Synthetic routes of ligands and their complexes are shown in scheme 1.

As previously described for related mixed-ligand $V^{IV}O$-complexes [15–17], IR spectra show absorptions at 3500–3470 cm^{-1} for (–OH), at 2951–3069 cm^{-1} for aromatic (C–H), at 1682–1697 cm^{-1} for aromatic (COOH), at 1597–1618 cm^{-1} for azomethine (–CH=N) and (C=C), at 1457–1570 cm^{-1} for azomethine group (C=C), and at 1217–1242 cm^{-1} for (C–O) [15–19, 27]. In IR spectra of complexes, the absorption of the azomethine (–CH=N) was reduced 17–18 cm^{-1} compared with the ligands, confirming coordination of azomethine (–CH=N) [16, 28, 29]. The strong (VO) band at 965 cm^{-1} could be clearly identified for the complexes [16, 17].

Electronic spectra of complexes and ligands are shown in table 1. Complexes **1** and **2** show an intense band at 264.5 nm assignable to π–π^* transition of aromatic rings of phenanthroline [16, 30–32]. A medium band is observed near 400 nm, attributed to a ligand-to-metal charge-transfer (LMCT) from a *p*-orbital on the ligand oxygen to the empty *d*-orbital of vanadium [24, 29]. Bands in the region 748.5 and 772.0 nm of low extinction coefficient values have been assigned to metal $d \rightarrow d$ transfer. Bands in the UV-Vis region (320–350 nm) are assignable to intraligand transitions of the Schiff base [30–33]. Five- and six-coordinate complexes of oxovanadium(IV) are usually square pyramidal/trigonal bipyramidal and distorted octahedral, respectively [24, 34, 35]. From the above spectral data, the Schiff bases bond through the phenolate oxygen, imine nitrogen, and carboxyl oxygen leaving the carboxyl as a pendant group. These complexes have square-pyramidal geometry around the central V(IV) [17, 24, 31–35]. This is also supported by the magnetic moment of 1.69–1.73 BM observed for five-coordinate VO(IV) complexes [24, 31]. Suggested structures of the complexes are given in scheme 1.

^1H NMR spectra of Schiff bases showed peaks of hydroxyl (OH), carboxyl (COOH), imine (CH=N) proton, and (CH_3O–) [35, 36]. However, in the ^1H NMR spectra of complexes, the peaks of (COOH) and hydroxyl (OH) were not observed, affirming that the ligand was coordinated to metal [18, 37]. In ES-MS spectra, Schiff bases showed

Table 1. Electronic spectral data of the complexes and ligands.

Compound	$\pi \rightarrow \pi^*$ λ_{max} (nm)	$n \rightarrow \pi^*$ λ_{max} (nm)	LMCT λ_{max} (nm)	$d \rightarrow d$ λ_{max} (nm)
MOSAA	258.0	342.5		
SAA	264.5	347.5		
VO(SAA)(p)	265.5	386.5	398.5	748.5
VO(MOSAA)(p)	264.5	324.0	391.5	772.0

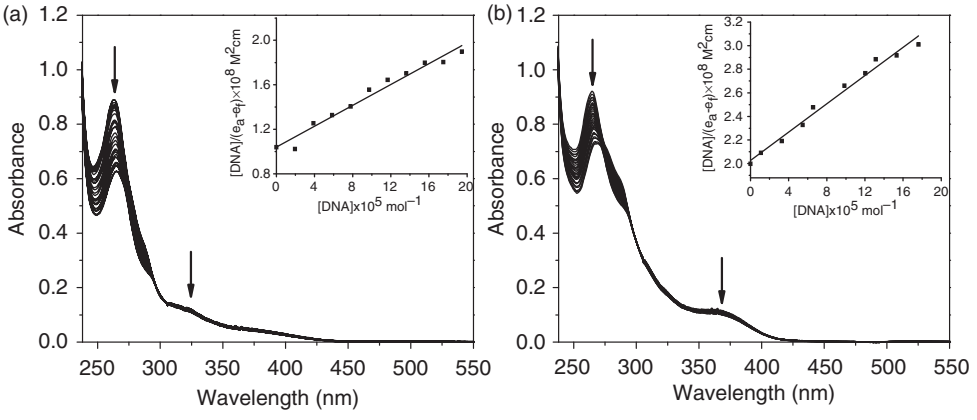

Figure 1. Absorption spectral trace of **1** (a) and **2** (b) on addition of CT-DNA in Tris-HCl buffer A. [V] = 20 μmol L^{-1}. Arrows show the decreasing absorbance with the increasing amounts of CT-DNA. Inset: plots of [DNA]/($\varepsilon_a - \varepsilon_f$) *vs.* [DNA] for the titration of [V] with CT-DNA.

peaks at *m*/*z* 242.0 ($[M+1]^+$) (SAA) and 272.0 ($[M+1]^+$) (MOSAA), respectively. The complexes showed peaks at *m*/*z* 487.0 ($[M+1]^+$) (**1**) and 517.0 ($[M+1]^+$) (**2**), respectively. Elemental analysis, UV-Vis, ES-MS, IR, and ^{1}H NMR results of all the compounds are in agreement with the expected structures. All of the compounds are neutral and non-conducting in DMF.

3.2. *DNA-binding studies*

3.2.1. Electronic absorption titration. Electronic absorption spectroscopy is one of the most common techniques to monitor the interaction of complexes with DNA. Complexes bound to the base pairs of DNA usually result in hypochromism and bathochromism, which is correlated with the stacking interaction between planar aromatic chromophore of complexes and the base pairs of DNA [38, 39]. The extent of the hypochromism is consistent with strength of intercalative binding interaction [9, 40–42].

The electronic absorption spectra of **1** and **2** in the absence and presence of CT-DNA are shown in figure 1. Upon increasing CT-DNA concentration, the hypochromism and bathochromic shift for **1** at 264.5 nm are 29.5% and 3 nm, respectively. However, under the same conditions, with increasing CT-DNA concentration, **2** exhibits hypochromism

of about 20.9%, and with a red shift of 2.5 nm at 273 nm. According to previous reported results [39, 41], we believe that **1** and **2** are most likely to bind with DNA through a stacking interaction between the aromatic chromophore of the ligands and the base pairs of DNA.

In order to compare quantitatively the binding strength of these two complexes with DNA, the intrinsic binding constant K_b was calculated by monitoring changes of absorbance in the ligand transfer bands, with increasing amounts of CT-DNA. The intrinsic binding constant K_b obtained for **1** and **2** were 4.50×10^4 $(\text{mol L}^{-1})^{-1}$ and 2.95×10^4 $(\text{mol L}^{-1})^{-1}$, respectively. Such values of intrinsic binding constants indicate that the interaction of **1** and **2** with DNA are weaker than reported complexes such as [VO(dbdppo)(bpy)](SO_4), [VO(dbdppo)(phen)](SO_4), and other systems [17, 8, 33], suggesting that the interaction of **1** and **2** with DNA are medium strength intercalation. The difference may be due to steric hindrance of the phenolate group. To fully understand the mechanism involved in the interaction of these two complexes with DNA, further investigation will be needed. The K_b value of **1** is larger than that of **2**, due to the different substituents in the ligands. The electron-pushing substituent (CH_3O– in SAA for **2**) on the intercalative ligand may decrease the DNA-binding affinity of the original complex [11, 18]. The results indicate that the DNA-binding affinities of oxovanadium complexes correlate with electronic effects of their intercalative ligands.

3.2.2. Fluorescence spectroscopic studies. The emission spectra of the complexes in the absence and presence of CT-DNA in Tris buffer A at room temperature are shown in figure 2. The emission intensity of **1** and **2** increase with increasing concentrations of CT-DNA, growing about 0.78 and 0.73 times for **1** and **2** at 602 nm, respectively. These values were larger than those of complexes alone and the [DNA]/[V] ratios are 8.75 : 1 and 6.81 : 1 for **1** and **2** at 602 nm after saturation of their emission intensities. This implies that these two complexes intercalate into the base pairs of the DNA helix. The enhancement may be due to the hydrophobic environment inside the DNA helix reducing the accessibility of water to the complex and complex mobility is restricted at

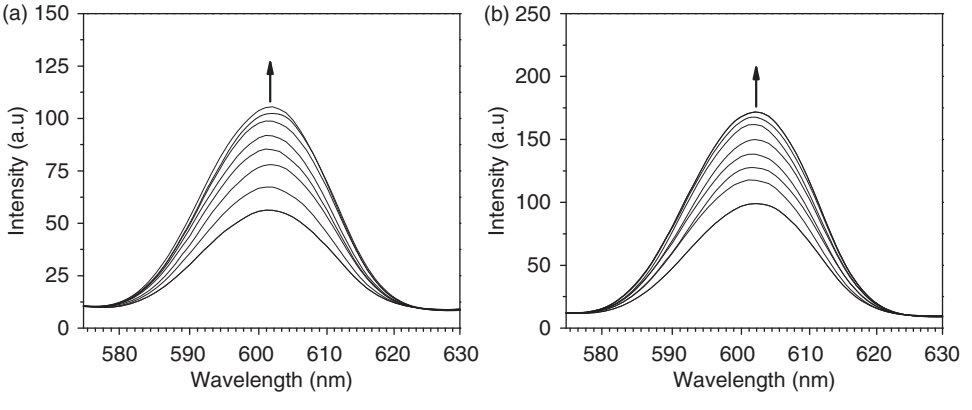

Figure 2. Emission spectra of **1** (a) and **2** (b) in Tris-HCl buffer A in the absence and presence of CT-DNA. [V] = 20 μmol L^{-1}. Arrows show the increasing intensity with increasing concentrations of DNA.

the binding site [17, 42]. The enhancement of emission intensities of both complexes indicates that the complexes were protected by the hydrophobic environment of DNA from water, leading to decrease of the vibrational modes of relaxation [42]. It also shows that **1** interacts with DNA more strongly than **2**, consistent with the above absorption spectra results.

3.2.3. Viscosity measurements. In the absence of crystallographic structural data or NMR spectra [24, 25], viscosity measurements that are sensitive to length change of DNA are regarded as the most critical tests of binding mode in solution. Intercalation of complexes into the base pairs of DNA leads to lengthening of the DNA helix as base pairs are separated to accommodate the binding ligand, resulting in an increase in viscosity of the DNA solution [43]. In contrast, partial and/or non-classical intercalation of ligand may bend or twist the DNA helix leading to a decrease in its effective length and, concomitantly, its viscosity [44, 45]. To further clarify the nature of the interaction between both complexes and DNA, viscosity measurements were carried out. The effects of **1** and **2** on the viscosity of CT-DNA are given in figure 3. Upon increasing concentrations of **1** and **2**, the relative viscosity of CT-DNA increases gradually. These results suggest that these two complexes bind to CT-DNA through intercalation modes [46, 47].

3.2.4. Thermal denaturation studies. DNA melting experiments are usually used to study extent of interaction. Figure 4 shows the changes of melting temperature of CT-DNA in the absence and presence of **1** and **2**. The melting temperature T_m was determined from the hyperchromic effect on the absorption of DNA base pairs ($\lambda = 260$ nm) resulting from the double-stranded DNA gradually dissociating to single strands with increasing temperature. The T_m of CT-DNA in the absence of the

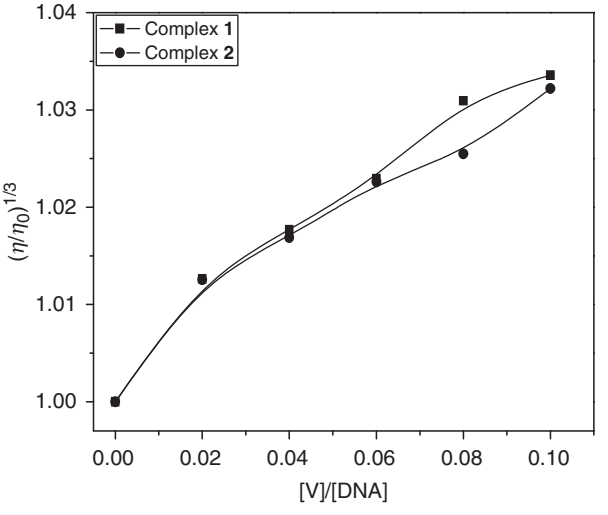

Figure 3. Effects of increasing amounts of **1** (■) and **2** (●) on the relative viscosity of CT-DNA at 28(±0.1)°C. [DNA] = 0.40 mmol L^{-1}.

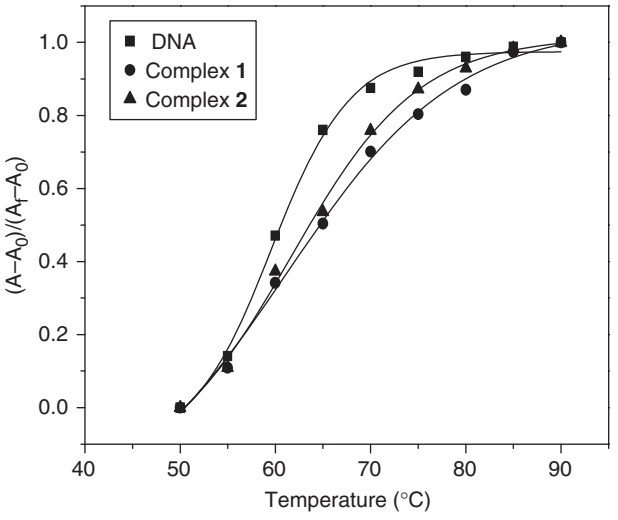

Figure 4. Thermal denaturation of CT-DNA in the absence (■) and presence of **1** (●) and **2** (▲). [V] = 20 μmol L^{-1}, [DNA] = 80 μmol L^{-1}.

complexes was 60.7°C. The observed T_m in the presence of **1** and **2** were 64.8°C and 63.7°C, respectively. The moderate increase in T_m (ΔT_m are 4.1°C and 3.0°C for the two complexes) were comparable to those observed for classical intercalators and lend strong support for their binding with DNA in intercalative modes [19, 48–50]. The results also reveal that **1** has a larger DNA-binding affinity than **2**.

3.3. *DNA cleavage*

Cleavage reactions of **1** and **2** toward plasmid DNA were studied by agarose gel electrophoresis. When circular plasmid DNA is subjected to electrophoresis, relatively fast migration is observed for the intact supercoiled form (Form I). If scission occurs on one strand (nicking), the supercoil form will relax to generate a slower moving open circular form (Form II). If both strands are cleaved, a linear form (Form III) that migrates between Forms I and II will be generated [51, 52].

In figure 5, the gel electrophoresis pattern of pBR322 DNA is shown after incubation with **1** and **2** at 37°C for 1 h in the dark. No DNA cleavage was observed for negative control (lane 1) and/or (lane 2). In the presence of **1** and **2** with 30 mmol L^{-1} H_2O_2 (lanes 3–5 and 8–10, respectively), plasmid DNA was nicked as is evident from the formation of Form II. These results indicate that the two oxovanadium complexes can degrade pBR322 DNA through oxidative cleavage in the presence of H_2O_2.

To study the cleavage mechanism of pBR322 DNA induced by **1** and **2**, the DNA cleavage experiment has been carried out in the presence of L-histidine (lanes 6 and 11) and DMSO (lanes 7 and 12). In the presence of L-histidine, a singlet oxygen quencher, the inhibition of DNA cleavage was not observed under the same conditions, whereas, complete inhibition of DNA cleavage occurred in the presence of hydroxyl radical scavenger DMSO (lanes 7, 12), suggesting that $^{\bullet}OH$ radical is likely the reactive species

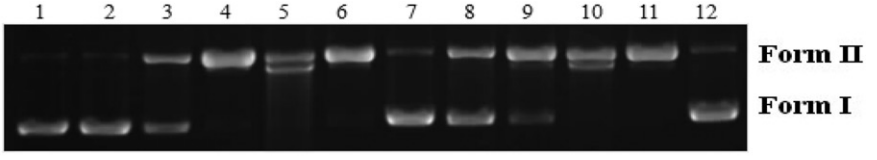

Figure 5. Cleavage of pBR322 DNA by **1** and **2** (15–60 μmol L^{-1}) in the absence and presence of H_2O_2 (30 mmol L^{-1}) in buffer B (pH 7.2). Lane 1, DNA control; lane 2, DNA + H_2O_2 (30 mmol L^{-1}); lane 3, DNA + **1** (15 μmol L^{-1}) + H_2O_2 (30 mmol L^{-1}); lane 4, DNA + **1** (30 μmol L^{-1}) + H_2O_2 (30 mmol L^{-1}); lane 5, DNA + **1** (60 μmol L^{-1}) + H_2O_2 (30 mmol L^{-1}); lane 6, DNA + **1** (30 μmol L^{-1}) + H_2O_2 (30 mmol L^{-1}) + L-histidine (0.02 mol L^{-1}); lane 7, DNA + **1** (30 μmol L^{-1}) + H_2O_2 (30 mmol L^{-1}) + DMSO (2 μL); lane 8, DNA + **2** (15 μmol L^{-1}) + H_2O_2 (30 mmol L^{-1}); lane 9, DNA + **2** (30 μmol L^{-1}) + H_2O_2 (30 mmol L^{-1}); lane 10, DNA + **2** (60 μmol L^{-1}) + H_2O_2 (30 mmol L^{-1}); lane 11, DNA + **2** (30 μmol L^{-1}) + H_2O_2 (30 mmol L^{-1}) + L-histidine (0.02 mol L^{-1}); lane 12, DNA + **2** (30 μmol L^{-1}) + H_2O_2 (30 mmol L^{-1}) + DMSO (2 μL).

Table 2. The IC_{50} values for SAA, MOSAA, **1**, and **2** against Ag8.653 and U251 cell lines.

	IC_{50} (μmol L^{-1})	
Compounds	Ag8.653	U251
Cisplatin	0.002 ± 0.001	0.005 ± 0.001
SAA	2.5 ± 0.1	12 ± 1
MOSAA	19 ± 4	32 ± 3
1	0.018 ± 0.006	0.038 ± 0.007
2	0.26 ± 0.07	0.29 ± 0.06

for cleavage. This may be explained by generation of $^{\bullet}OH$ radicals obtained from the oxidation of VO^{2+} in the presence of H_2O_2 through the reaction as follows: ($VO^{2+} + H_2O_2 \rightarrow VO_2^+ + {}^{\bullet}OH + H^+$) [2, 18, 52]. According to previously reported results [2], we believe that DNA cleavage may be closely related to oxidation of vanadyl ions of oxovanadium complexes. Further studies are currently underway to clarify the cleavage mechanism.

3.4. *Cytotoxic assay in vitro*

The effects of **1** and **2** were examined on myeloma cells (Ag8.653) and gliomas cells (U251) cell lines using the MTT assay [14, 17], a colorimetric determination of cell viability during *in vitro* treatment with a drug. The IC_{50} values were derived after the selected tumor cells incubated for 48 h in the presence of **1** and **2** and cisplatin in various concentrations. The IC_{50} values of the vanadium complexes and cisplatin for growth inhibition of Ag8.653 and U251 cells are given in table 2. The histograms of cell viability assay for different compounds against selected tumor cells are shown in figure 6. As shown in table 1 and figure 6, the antitumor activities of **1** and **2** are concentration-dependent and **1** ($IC_{50} = 0.018 \pm 0.006$, 0.038 ± 0.007) possessed more inhibitory effect against the two cell lines. The antiproliferative activity with increasing concentrations of **1** is shown in figure 7. Comparing the cytotoxicity of the ligands and

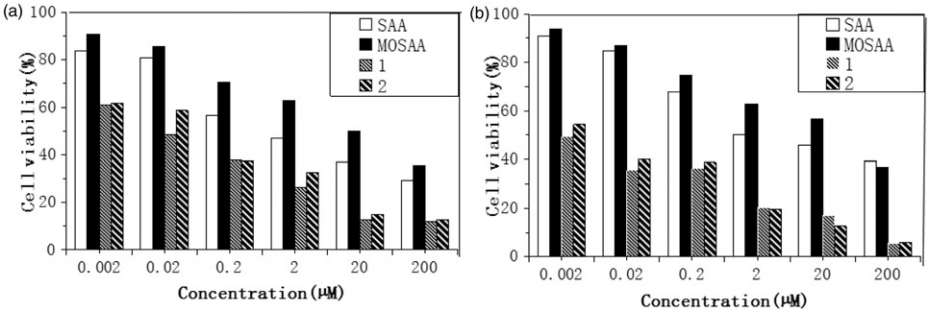

Figure 6. Cell viability of **1** and **2** on Ag8.653 and U251 cell proliferation *in vitro*. Each data point is the mean ± standard error obtained from three independent experiments.

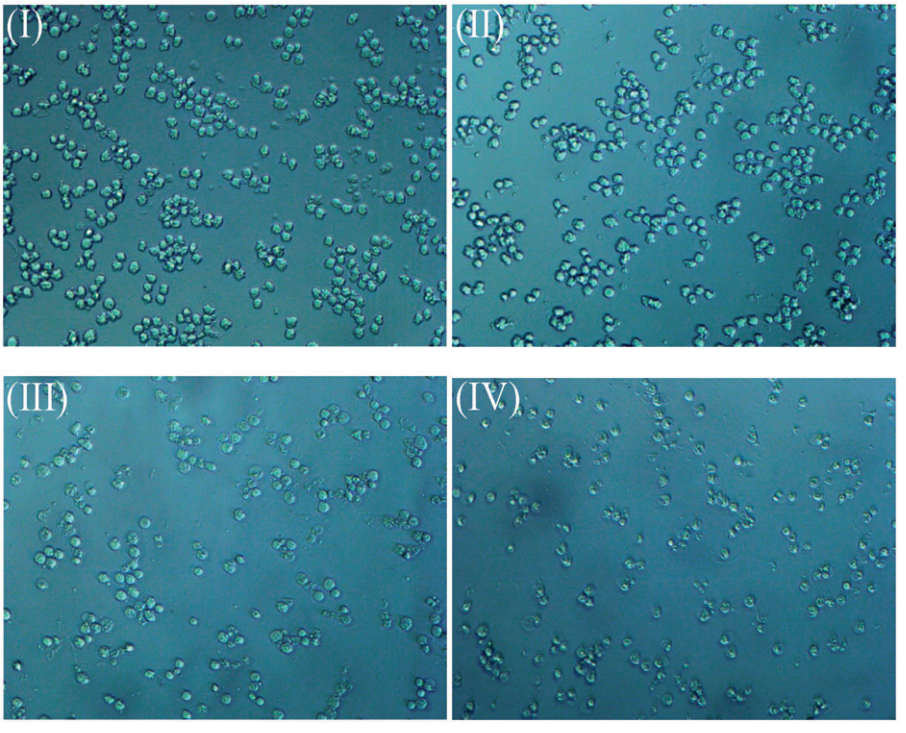

Figure 7. Micrograph of the myeloma tumor (Ag8.653) cell line after treatment for 48 h in the absence I (the control) and presence of different concentrations of **1**; II: [V] = 0.002 μmol L^{-1}; III: [V] = 0.02 μmol L^{-1}; IV: [V] = 0.2 μmol L^{-1}.

corresponding complexes, it can be concluded that antitumor activities against selected tumor cell lines have been remarkably enhanced when ligands coordinate with vanadium [16, 17, 53]. Complexes **1** and **2** exhibit *in vitro* cytotoxicity against the selected cells lines, but lower than that of cisplatin which was determined in this work through the same technique.

4. Conclusion

Two unsymmetrical oxovanadium complexes, [VO(SAA)(phen)] (**1**) and [VO(MOSAA)(phen)] (**2**), have been synthesized and characterized by elemental analysis, UV-Vis, ES-MS, IR, and ^{1}H NMR spectroscopy. The DNA-bindings of these complexes were investigated by spectroscopic methods, viscosity measurements, and thermal denaturation. The results show that **1** and **2** bind to CT-DNA in intercalation mode. The DNA-binding affinity of **1** is larger than that of **2**. These oxovanadium complexes are capable of cleaving supercoiled plasmid DNA in the presence of H_2O_2. Both **1** and **2** have cytotoxic activities against Ag8.653 and U251 cell lines, with **1** possessing more inhibitory effect. Further investigation is required to study the possible cytotoxicity mechanisms of these two complexes.

Acknowledgments

We gratefully acknowledge financial support for this work by Guangdong Pharmaceutical University (No. 43540119), the National Key Research Project of China (No. 2011zx09102-001-31), and the National Natural Science Foundation of P.R. China (Nos 81102753 and 31070858).

References

[1] F.J. Chen, M. Xu, P.X. Xi, H.Y. Liu, Z.Z. Zeng. *Spectrochim. Acta, Part A: Mol. Biomol. Spectrosc.*, **81**, 21 (2011).
[2] L. Leelavathy, S. Anbu, M. Kandaswamy, N. Karthikeyan, N. Mohan. *Polyhedron*, **28**, 903 (2009).
[3] E.K. Efthimiadou, N. Katsaros, A. Karaliota. *Bioorg. Med. Chem. Lett.*, **17**, 1238 (2007).
[4] B.T. Thaker, K.R. Surati, C.K. Modi. *Russ. J. Coord. Chem.*, **34**, 25 (2008).
[5] A. Bishayee, A. Waghray, M.A. Patel. *Cancer Lett.*, **294**, 1 (2010).
[6] I.C. Mendes, L.M. Botion, A.V.M. Ferreira. *Inorg. Chim. Acta*, **362**, 414 (2009).
[7] J. Benitez, L. Becco, I. Correia. *J. Inorg. Biochem.*, **105**, 303 (2011).
[8] P.I. da S. Maia, F.R. Pavan, C.Q.F. Leite, S.S. Lemos, G.F. de Sousa, A.A. Batista, O.R. Nascimento, J. Ellena, E.E. Castellano, E. Niquet, V.M. Deflon. *Polyhedron*, **28**, 398 (2009).
[9] J.H. Hwang, R.K. Larson, M. Mahdi. *Inorg. Chem.*, **42**, 7967 (2003).
[10] W.X. Hu, W. Zhou, C.N. Xia, X. Wen. *Bioorg. Med. Chem. Lett.*, 2213 (2006).
[11] Y.J. Liu, J.C. Chen, F.H. Wu. *Transition Met. Chem.*, **34**, 297 (2009).
[12] A.A. El-Asmy, O.A. Al-Gammal, D.A. Saad, S.E. Ghazy. *J. Mol. Struct.*, **934**, 9 (2009).
[13] P.K. Sasmal, A.K. Patra, A.R. Chakravarty. *J. Inorg. Biochem.*, **102**, 1463 (2008).
[14] N. Shahabadi, S. Kashanian, M. Purfoulad. *Spectrochim. Acta, Part A: Mol. Biomol. Spectrosc.*, **72**, 757 (2009).
[15] J. Benítez, L. Guggeri, I. Tomaz, J. Costa Pesso, V. Moreno, J. Lorenzo, F.X. Avilés, B. Garat, D. Gambino. *J. Inorg. Biochem.*, **103**, 1386 (2009).
[16] J. Benítez, L. Guggeri, I. Tomaz, G. Arrambide, M. Navarro, J. Costa Pessoa, B. Garat, D. Gambino. *J. Inorg. Biochem.*, **103**, 609 (2009).
[17] J. Benítez, L. Becco, I. Correia, S.M. Leal, H. Guiset, J.C. Pessoa, S. Tanco, P. Escobar, V. Moreno, B. Garat, D. Gambino. *J. Inorg. Biochem.*, **105**, 303 (2011).
[18] J.Z. Lu, Y.F. Du, H.W. Guo. *J. Coord. Chem.*, **64**, 1229 (2011).
[19] Y.F. Du, J.Z. Lu, H.W. Guo, J. Jiang. *Transition Met. Chem.*, **35**, 859 (2010).
[20] P. Zhao, L.C. Xu, J.W. Huang, B. Fu, H.C. Yu, L.N. Ji. *Biophys. Chem.*, **135**, 102 (2008).
[21] P. Zhao, L.C. Xu, J.W. Huang, B. Fu, H.C. Yu, L.N. Ji. *Spectrochim. Acta, Part A: Mol. Biomol. Spectrosc.*, **71**, 1216 (2008).
[22] P. Zhao, L.C. Xu, J.W. Huang, B. Fu, H.C. Yu, L.N. Ji. *Bioorg. Chem.*, **36**, 278 (2008).

[23] X.L. Liang, L.F. Tan, W.G. Zhu. *DNA Cell Biol.*, **30**, 61 (2011).
[24] L.Z. Li, Z.H. Guo, Q.F. Zhang, T. Xu, D.Q. Wang. *Inorg. Chem. Commun.*, **13**, 1166 (2010).
[25] Y.J. Liu, C.H. Zeng. *Eur. J. Med. Chem.*, **45**, 3087 (2010).
[26] C.Z. Li, J.G. Wu, L.F. Wang, R. Min. *J. Inorg. Biochem.*, **73**, 195 (1999).
[27] I. Dilovic, M. Rubcic, V. Vrdoljak, S.K. Pavelic, I. Piantanida, M. Cindric. *Bioorg. Med. Chem.*, **16**, 5189 (2008).
[28] A.A. Nejo, G.A. Kolawole, A.R. Opoku, J. Wolowska, P. O'Brien. *Inorg. Chim. Acta*, **62**, 3993 (2009).
[29] S. Gorelsky, G. Micera, E. Garribba. *Chem. Eur. J.*, **16**, 8167 (2010).
[30] P.K. Sasmal, A.K. Patra, A.R. Chakravarty. *J. Inorg. Biochem.*, **102**, 1464 (2008).
[31] N. Raman, A. Selvan. *J. Mol. Struct.*, **985**, 173 (2011).
[32] S.K. Dutta, S.B. Kumar, S. Bhattacharyya. *Inorg. Chem.*, **36**, 4954 (1997).
[33] M. Nakai, M. Obata, F. Sekiguchi, M. Kato, M. Shiro, A. Ichimura, I. Kinoshita, M. Mikuriya, T. Inohara, K. Kawabe, H. Sakurai, C. Orvig, S. Yano. *J. Inorg. Biochem.*, **98**, 105 (2004).
[34] A.A. Nejo, G.A. Kolawole, A.R. Opoku. *Inorg. Chim. Acta*, **62**, 3411 (2009).
[35] Z.H. Chohan, S.H. Sumrra, M.H. Youssoufi, T.B. Hadda. *Eur. J. Med. Chem.*, **45**, 2739 (2010).
[36] J. Costa Pessoa, I. Cavaco, I. Correia, I. Tomaz, M.T. Duarte, P.M. Matias. *J. Inorg. Biochem.*, **80**, 35 (2000).
[37] G. Micera, V.L. Pecoraro, E. Garribba. *Inorg. Chem.*, **48**, 5790 (2009).
[38] N. Butenko, A.I. Tomaz, O. Nouri, E. Escribano, V. Moreno, S. Gama, V. Ribeiro, J.P. Telo, J. Costa Pesssoa, I. Cavaco. *J. Inorg. Biochem.*, **103**, 622 (2009).
[39] P.K. Sasmal, A.K. Patra, M. Nethaji, A.R. Chakravarty. *Inorg. Chem.*, **46**, 11112 (2007).
[40] G. Verquin, G. Fontaine, M. Bria, E. Zhilinskaya, E. Abi-Aad, A. Aboukais, B. Baldeyrou, C. Bailly, J. Bernier. *J. Biol. Inorg. Chem.*, **9**, 345 (2004).
[41] H.L. Wu, K. Li, T. Sun. *Transition Met. Chem.*, **36**, 21 (2011).
[42] W.J. Mei, Y.Z. Ma. *Transition Met. Chem.*, **31**, 277 (2006).
[43] J.G. Liu, O.L. Zhang, X.F. Shi, L.N. Ji. *Inorg. Chem.*, **40**, 5045 (2001).
[44] L.N. Ji, X.H. Zhou, J.G. Liu. *Coord. Chem. Rev.*, **216–217**, 513 (2001).
[45] R.J. Fiel, B.R. Munson. *Nucleic Acids Res.*, **8**, 2835 (1980).
[46] E.C. Long, J.K. Barton. *Acc. Chem. Res.*, **23**, 271 (1990).
[47] D. Suh, J.B. Chaires. *J. Bioorg. Med. Chem.*, **3**, 723 (1995).
[48] S. Satyanarayana, J.C. Dabrowiak, J.B. Chaires. *Biochemistry*, **32**, 2573 (1993).
[49] T. Uno, K. Hamasaki, M. Tannigawa, S. Shimabayashi. *Inorg. Chem.*, **36**, 1676 (1997).
[50] C.V. Kumar, E.H. Asuncion. *J. Am. Chem. Soc.*, **115**, 8547 (1993).
[51] J.K. Barton, A.L. Raphael. *J. Am. Chem. Soc.*, **106**, 2466 (1984).
[52] Q.L. Zhang, J.G. Liu, H. Li. *Inorg. Chim. Acta*, **339**, 34 (2002).
[53] H.B. Brooks, F. Sicillo. *Inorg. Chem.*, **10**, 2530 (1971).